



ELSEVIER

Biophysical Chemistry 105 (2003) 471–494

Biophysical  
Chemistry

www.elsevier.com/locate/bpc

## Conformational complexity of melatonin in water and methanol

Donald D. Shillady<sup>a,\*</sup>, Charles M. Castevens<sup>a,b</sup>, Carl Trindle<sup>c</sup>, Jeffrey Sulik<sup>a</sup>,  
Paula Klonowski<sup>a</sup>

<sup>a</sup>Department of Chemistry, Virginia Commonwealth University, Box 842006, Richmond, VA 23284-2006, USA

<sup>b</sup>Department of Academic Technology, Virginia Commonwealth University, Box 842030, Richmond, VA 23284-2030, USA

<sup>c</sup>Department of Chemistry, University of Virginia, Charlottesville, VA 22904-4319, USA

Received 18 September 2002; received in revised form 19 December 2002; accepted 19 December 2002

### Abstract

The magnetic circular dichroism (MCD) spectra of melatonin in water and methanol solutions is compared to the MCD spectra of indole and five melatonin conformations observed in low temperature jet spectroscopy. Based on a survey of indole compounds using Slater type orbitals-6G(d,p) and B3LYP/6-31G(d) energies, and CNDO/S-D calculations of MCD spectral bands, a dominant structure with a water molecule bridging the amide-keto oxygen and indole N–H atoms is proposed as the best fit for the MCD of aqueous melatonin. In methanol an additional band appears at 310 nm which is supported only by solvated structures in which the alkyl-amide arm is extended away from the indole moiety.

© 2003 Elsevier Science B.V. All rights reserved.

**Keywords:** CNDO/S-D; Complexity; Conformation; Magnetic circular dichroism; Melatonin; Solvation

### 1. Introduction

Measurement of optical activity has long been a technique applied to structural questions in biological systems at the molecular level, but usually for nearly rigid molecules. Kauzmann's early review on optical rotatory power [1] influenced the development of the theory of optical rotation for over 50 years. Prof. Kauzmann has also inspired a number of his former students to continue this work and certainly has formed a foundation

for such work in this laboratory. Kauzmann later [2] extended the first formulation of the theory of optical activity [3] to the more general case of optical activity induced by a magnetic field [4]. Description of the full frequency dependence of magnetically induced optical activity was reported later by Stephens [5,6]. A variety of theoretical models have been developed for description of optical activity such as the 'vibrating electron model' of Rosenfeld later extended by Condon [7] and the 'one-electron model' of Gorin [8,9], which probably reached the most highly developed form in work by Kwok [10]. Other work with this approach was applied to dipeptides by Schellman et al. [11,12]. All of these treatments considered localized regions of chromophores perturbed by

\*Corresponding author. Fellow of the Center for the Study of Biological Complexity, Virginia Commonwealth University, Richmond, VA, USA. Tel.: +1-804-828-7508; fax: +1-804-828-8599.

E-mail address: dshillad@mail1.vcu.edu (D.D. Shillady).

asymmetric arrangement of vicinal groups. These theories are treated in the text by Kauzmann [13] both from a classical view and using quantum mechanics in what is still the most complete treatment of optical activity available.

A slightly different concept of optical activity was introduced by Tinoco [14] for delocalized  $\pi$ -electron systems such as hexahelicene. That work employed a true molecular orbital method in which the optical transitions might be delocalized over an asymmetric molecular framework. An all-valence-electron method was then developed by Richardson et al. [15,16] using approximate molecular orbitals for valence electrons [17], addressing the problems posed in the 1940 review by Kauzmann regarding methylcyclopentanone [1] as a case where an asymmetric perturbing group is not directly attached to the carbonyl chromophore. This same formalism was used to examine the magnetic circular dichroism (MCD) of indole, tryptophan and serotonin [18] and the conformational dependence of the circular dichroism (CD) of 1-methyl-indane [19]. This method depends on the use of configuration interaction of single-excitations (CIS) [20] and semiempirical wavefunctions adjusted to fit the  $A_{1g} \rightarrow B_{2u}$  band of benzene [21].

The methods described above all treat isolated gas phase molecules while most measurements are made on systems in aqueous solution. Recent advances in computational and experimental methods make possible the investigation of solute–solvent clusters. Work in this laboratory has focused on solvent clusters [22] and solvent interactions [23]. Models of solvated species in bulk solutions can also be related to detailed spectroscopic analysis of electrospray mass spectrometry [24] and low temperature supersonic jet expansion techniques [25–31].

These new methods offer highly detailed spectroscopic information regarding specific conformations of flexible biomolecules and provide data for improved models of amphiphilic protein residues such as tryptophan in membrane proteins [32]. Spectroscopic studies of gas phase analogs of amino acids and their clusters with water are necessary to develop more accurate treatments of

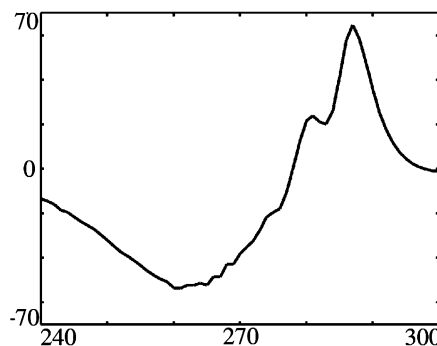


Fig. 1. MCD of Indole in water, 1.35 mg/ml, 1 nm resolution, 1 cm cell, 15 kG.

residues such as Arg, Lys, Trp and Tyr which are both polar and hydrophobic and likely to be important on the surface of membrane proteins.

The most recent work from Zwier's laboratory [30] is a highly detailed analysis of low temperature gas phase conformers of melatonin. The rich detail of this new work provides insight to a previously noted differences between the MCD spectrum of serotonin and that of indole, the MCD spectrum of melatonin is also quite different from that of indole. The recent work of Zwier [30] shows that the 5-methoxy substitution of indole in melatonin effects a slight red shift of the first  $\pi \rightarrow \pi^*$  band of the ultraviolet (UV) absorption spectrum. This agrees with a previous observation by Sprinkel et al. [18] that 5-hydroxy substitution of indole in serotonin produces a small red shift. More puzzling is the fact that while indole has a sharp, well-defined MCD band at approximately 287 nm as shown in Fig. 1, both serotonin [18] and melatonin [30], shown in Fig. 2 with the first derivative in Fig. 3, have a broad, featureless band extending from approximately 280 to 310 nm. In this work we compare the MCD spectrum of melatonin to that of indole using new information provided by Zwier [30], but it is now apparent that a similar broadening effect is probably operative in the MCD band of serotonin near 300 nm.

The biological importance of substituted-indole compounds can be appreciated by the large number of studies on reserpine, serotonin, melatonin, hun-

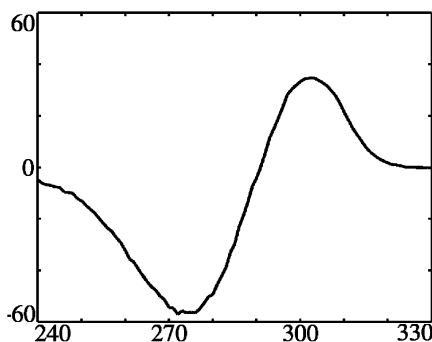


Fig. 2. MCD of melatonin in water, 0.9475 mg/ml, 1 nm resolution, 1 cm cell, 15 kG, average of 9 scans.

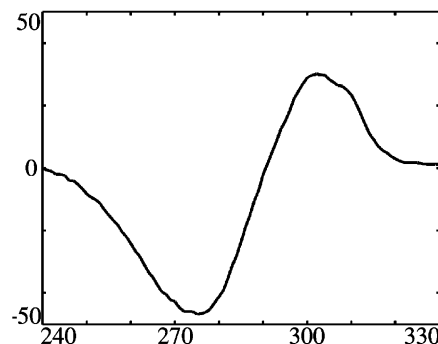


Fig. 4. MCD of melatonin in methanol, 0.825 mg/ml, 1 nm resolution, 1 cm cell, 15 kG, average of 9 scans.

dreds of plant hormones and more recently the development of the kenpaullone anti-cancer drug [33], isolation of antifungal compounds from deep water sponges [34] and studies of multiple melatonin binding sites [35]. MCD is a tool well suited for study of substituted indoles due to an intense electronic band near 290 nm [36] which is sensitive to conformation of substituents.

The obvious difference between rigid and alkyl-substituted indoles is that alkyl-substitution brings conformational complexity, yet is more amenable to detailed study than proteins which have far more complexity. The calculation of the optical activity of 1-methyl-indane [19,37] should have alerted those using optical activity for structural analysis to what might be termed ‘the problem of conformational complexity’. It is now clearly

established by analysis of the gas phase spectra that in 1-methyl-indane there is a dynamic equilibrium between axial and equatorial conformations of the methyl group. Further complications may arise from solvent interactions, which might change conformer populations and thus alter the observed spectra of solutions from gas phase structures.

With recent advances in experimental and computational methods it is now possible to characterize melatonin and other important hormone molecules for which both solvation and conformational energy play roles in determining the predominant conformation(s). Considering the interest in the biological function of melatonin [38–40] it is useful to relate the recent conforma-

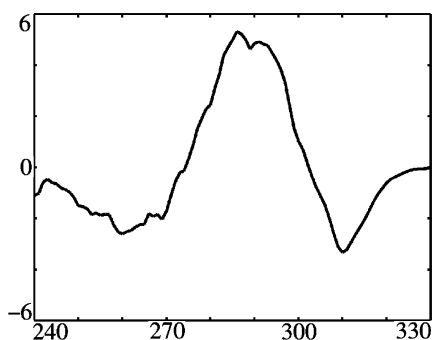


Fig. 3. First derivative of Fig. 2.

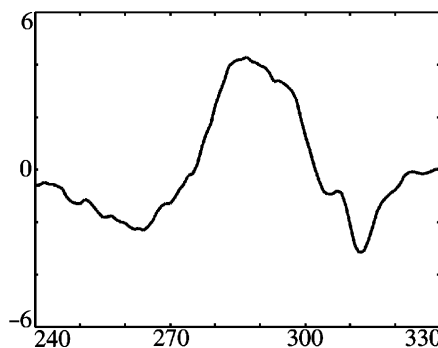


Fig. 5. First derivative of Fig. 4.

tional work from Zwier's laboratory [30] to MCD, the most general form of optical activity.

## 2. Materials and methods

### 2.1. Experimental

Indole (99%) and melatonin (99.5%) were purchased from Aldrich Chemical Co. (Milwaukee, WI) and used as received to make solutions in deionized water and 99.9% spectrophotometric grade methanol. Dissolution was aided by the use of ultrasonification. The MCD spectra were measured using a JASCO J600 spectropolarimeter equipped with a room temperature electromagnet operated at 15 kG with a pole gap suitable for a 1 cm path quartz cell and cooled with refrigerated water at 23 °C. In order to achieve smooth spectra, the resolution was set at 1 nm. The computer interface to the JASCO J600 provides software options for subtraction of solvent baseline, repetitive scan averaging and presentation of the first derivative of spectral scans, all of which were used in this work. Scan rates and settings were used as recommended in the manual accompanying the JASCO J600. Repetitive scans were accumulated as indicated in the captions to the figures. The sign convention was checked against previous spectra published from this laboratory. The direction of the axial electromagnetic field was set so that the MCD peak of tryptophan was positive at 290 nm [36].

### 2.2. Computational

The computational modeling was carried out on a 16 CPU Origin 2000, a 2 CPU Origin 200 and three single-processor O2 computers from Silicon Graphics (SGI), along with a 32 CPU Beowulf cluster and a 64 CPU ServeLinux Beowulf cluster, all at Virginia Commonwealth University, plus an 8 CPU PQS cluster and three desktop computers at the University of Virginia. SPARTAN [41], a molecular orbital modeling program, permitted the systematic generation of low-energy conformers of melatonin by enumerating torsion angles. The program generated approximately 80 low-energy

structures in a preliminary PM3 semiempirical survey. The 20 lowest energy structures were refined with Slater type orbitals (STO)-3G optimizations within SPARTAN. Further geometry optimizations utilized GAUSSIAN98 [42] and GAMESS [43]. GAUSSIAN98 also provided the time-dependent density functional theory (TD-DFT) option to estimate low-lying UV absorption energies. The details of the TD-DFT method used in GAUSSIAN98 are readily accessible [44,45].

Much of the project used substantially modified programs derived from several sources. The MCD program used in previous research [17,18] was recently enlarged to treat up to 1500 atoms and 2500 valence shell orbitals in the CNDO/S formalism [21]. This semiempirical method is extremely fast for large molecules due to the use of the zero-differential-overlap (ZDO) approximation in the time-consuming evaluation of the coulomb and exchange integrals in the CIS step. The excited states are represented by single excitations from the closed shell ground state; this is the CIS approximation [20]. The CIS method is well known to overestimate excitation energies. The first CNDO/S method [21] compensated for this by multiplying the  $\pi \rightarrow \pi^*$  excitation energies by 0.585.

In order to include all two-center matrix elements in the optical activity calculations, the CNDO/S ZDO-wavefunction is deorthogonalized using an inverse Löwdin transformation [46] so that the molecular orbitals resemble *ab initio* minimum basis orbitals. These deorthogonalized molecular orbitals (CNDO/S-D) are used in the estimation of electric and magnetic transition moments. In order to check the semiempirical results, the same algorithm was coded into an *ab initio* program under development in this laboratory based on Gaussian lobe orbitals, PCLOBE [47]. PCLOBE uses a full two-electron transformation in the configuration interaction step. Note the original 1970 MCD program [17] used STO. In order to interface Gaussian calculations with the STO-basis program the original subroutines were inserted into PCLOBE to use (6G 1s/4G 2s) orbitals [48] and lobe-basis 4G 2p orbitals [49] as Gaussian mimics of the STO-basis.

Both the semiempirical CNDO/S-D MCD program and the Gaussian lobe ab initio program allowed 99 single-excitations plus the ground state. To compensate for the systematic overestimation of the excitation energies by CIS, the excitation energies from PCLOBE were scaled by 0.646. Thus, a calculation using a (6G 1s/4G 2s/4G 2p) basis where the 4G 2p is constructed from eight Gaussian spheres [49,50] with Clementi's best single zeta screening values [51] and a 4G 1s [48] for H with a screening constant of 1.20 was calibrated to the  $A_{1g} \rightarrow B_{2u}$  transition of benzene [52]. A standard text [53] gives this energy as 38 091/cm (equivalent to a wavelength of 262.53 nm). The scaling factor to fit the PCLOBE CIS energy to this transition is 0.646.

The present PCLOBE–CIS–MCD code employs a full two-electron transformation in the configuration interaction step, but the demands of the conversion of the atomic orbital repulsion integrals to the corresponding coulomb and exchange integrals over molecular orbitals made the use of this code impractical for more than 100 basis functions at this time. This limited ab initio calculations of the MCD spectral parameters to a minimum basis representation of the parent indole compound plus 1 or 2 water molecules. Although d-orbitals are known to improve the variational description of pi bonds [54], the use of a minimum basis without d-polarization functions for the MCD calculations was necessary due to the additional need to compute all six (Ex, Ey, Ez, Mx, My and Mz) transition moment matrices in the perturbation treatment of the Rigid Shift Model of MCD [5]. Nevertheless, this is still an ab initio all electron treatment in a minimum basis set.

The equations for the 'Rigid Shift' treatment of MCD [5] are given in Eqs. (1)–(6) to show that following the CIS, the electric and magnetic transition moments need to be computed in the linear combination of single-excitations from the ground state determinant as representations of excited states [55]. The philosophy of the rigid-shift-model is that the presence of an external magnetic field merely shifts the energies of the excited states according to a first-order perturbation interaction of the magnetic moments of those states with the

magnetic field. This approximation has been found to be valid for magnetic fields up to 50 000 G and certainly applies to the 15 000 G field used in this work. Here  $\langle a | \mathbf{m} | j_\lambda \rangle$  is the electric transition moment and  $\langle a | \boldsymbol{\mu} | j_\lambda \rangle$  is the magnetic transition moment for the  $(a \rightarrow j_\lambda)$  transition, in accordance with previous work from this laboratory.

For low symmetry molecules as here, the A-terms are negligible and no paramagnetic C-terms [5] occur when treating closed shell ground electronic states. Thus, the B-terms are the most general effect in the MCD spectra of molecules, but note that in Eq. (5) the sign of the spectral band is opposite to the value of the B-term. We note that Ball [56] has given a useful introduction to MCD spectroscopy with an opposite sign to Eq. (5), but we know that there at least two ways to reverse the sign of the spectra, first by reversing the direction of the magnetic field and second by adjusting the phase detection circuit by 180°. We choose to use the equations given by Stephens [5] and adjust our spectrometer to give a positive peak for tryptophan at 290 nm in agreement with Barth et al. [36]. In addition, the  $(B/D)$  ratio indicates the relative band strength of the Faraday B-term compared to the oscillator strength which is proportional to  $D^2$ . Dividing B by D also eliminates the electric units from the ratio, leaving  $(B/D)$  as bohr-magnetons/(cm<sup>-1</sup>). Although the  $(B/D)$  values seem small (CD is typically 10<sup>-5</sup> times the absorption), it should be noted that multiplication by the value of the magnetic field used here of 15 000 G yields much larger values which are measurable with modern amplification of the photomultiplier signal. The absorption band shape  $f^0$  in Eq. (6) could be a Gaussian as fitted to absorption or a lorentzian fitted to natural line width [13], but it is generally understood that the B-terms result in bands with finite width similar to absorption bands except that B-terms can be positive or negative.

$$A(a \rightarrow j) = \frac{1}{2} \sum_{\sigma} \sum_{\lambda} \text{Im} \left[ \langle a | \vec{m} | j_{\sigma} \rangle \times \langle j_{\lambda} | \vec{m} | a \rangle \langle j_{\sigma} | \vec{\mu} | j_{\lambda} \rangle \right] \quad (1)$$

$$B(a \rightarrow j) = \sum_{\lambda} \sum_{k \neq j} \text{Im} \left[ \langle a | \vec{m} | j_{\lambda} \rangle \langle k | \vec{m} | a \rangle \frac{\langle j_{\lambda} | \vec{\mu} | k \rangle}{(E_k - E_j)} + \langle a | \vec{m} | j_{\lambda} \rangle \langle j_{\lambda} | \vec{m} | k \rangle \frac{\langle k | \vec{\mu} | a \rangle}{(E_k - E_a)} \right] \quad (2)$$

$$D(a \rightarrow j) = \sum_{\lambda} \left| \langle a | \vec{m} | j_{\lambda} \rangle \right|^2 \quad (3)$$

$$k = \frac{2\pi^2 \alpha^2 N}{3\hbar n} D(a \rightarrow j) f^0(\omega) \quad (4)$$

$$\Delta k = \frac{4\pi^2 \alpha^2 N}{3\hbar n} \times \left\{ \frac{A(a \rightarrow j)}{\hbar} f'(\omega) - B(a \rightarrow j) f^0(\omega) \right\} \vec{H} \quad (5)$$

$$\int f^0(\omega) d\omega = 1 f'(\omega) = \frac{\partial f^0}{\partial \omega} \quad (6)$$

$$\int f'(\omega) d\omega = 0 \quad \int \omega f'(\omega) d\omega = -1$$

It was found that the present ab initio version of the MCD program PCLOBE was unable to treat more than 100 orbitals as required for the various conformations A, B, C, D and E of melatonin observed by Zwier's group [30] so that those conformers were treated only by the semiempirical CNDO/S-D method for the MCD bands. The energy of each conformation was calculated using the B3LYP local density approximation in the GAUSSIAN98 program with a 6-31G\* basis to include some electron correlation in the energies and the structure were optimized to within a root-mean-square gradient of 0.0003 hartrees/bohr. The conformations were also optimized using GAMESS with a STO-6G(d,p) basis set and only very slight geometrical changes were required to optimize the structures in the STO-6G(d,p) basis. Thus, the CNDO/S-D results are reported for the B3LYP/6-31G\* geometries.

### 3. Results

Table 1 presents the results calculated for the first few transitions for comparison with the MCD spectrum in Fig. 2 using the enlarged semiempirical program developed previously [17]. The ZDO oscillator strength  $f(\text{ZDO})$  uses the dipole length computed by including only one-center electric dipole matrix elements while the  $f(\text{d-vel})$  values include all two center terms in the dipole-velocity form of the transition moments; both are only qualitatively accurate since the wavefunctions are deorthogonalized CNDO/S orbitals [46]. It should be noted that if the wavefunction was exact the oscillator strengths would be equal whether calculated from the dipole length or the dipole velocity; the difference between the two values is a very sensitive measure of the accuracy of the wavefunction. The less-well-known magnetic matrix elements checked exactly with known values [57].

The ground state of melatonin is an electronic closed-shell singlet and the symmetry is C1 so there are no true A-terms or C-terms in the notation of Stephens [5]. The first transition at 317 nm for the protein data bank (PDB) structure (Fig. 14) is the nearly-forbidden  $n \rightarrow \pi^*$  transition of the amide group. The second band is also nearly-forbidden electrically, but has a large magnetic transition moment due to the in-plane N-sigma electrons at the indole N site being excited into the  $\pi^*$  system of the indole moiety (calculated to be at 286 nm). The signs of the first, second and third bands agree qualitatively with the experimental MCD spectrum. Transitions 4, 5 and 6 are indicated as strong  $\pi \rightarrow \pi^*$  transitions with large oscillator strengths, but good signal/noise was difficult to obtain experimentally at wavelengths less than 230 nm. Since the CNDO/S method was calibrated with the 0.585 factor for  $\pi^*$  states, the amide  $n \rightarrow \pi^*$  transition is predicted to be where such a transition should occur ( $\sim 320$  nm) for this structure in which the alkyl amide is extended away from the indole ring system. It will be important to note the wavelength accuracy of the CNDO/S method when the conclusion of this work will depend somewhat on matching predicted wavelengths to experiment for an unknown case.

Table 1  
MCD band assignments for melatonin (CNDO/S-D, 99 CI)

nm	$f(\text{ZDO})$	$f(\text{d-vel})$	$(B/D)$ , B.M./cm	Experimental, nm
Melatonin PDB geometry <sup>a</sup> (Fig. 14)				
317	0.00110	0.00075	−0.0000550	
286	0.01217	0.00299	−0.0002925	
251	0.26681	0.13479	0.0000184	
222	0.21946	0.08469	0.0000747	
212	0.28105	0.12705	−0.0000051	
205	0.00421	0.00687	−0.0003083	
203	0.42665	0.16371	−0.0001434	
Melatonin + (H <sub>2</sub> O) <sub>5</sub> <sup>b</sup> (Fig. 16)				
302	0.00087	0.00613	−0.0001401	(+)302
291	0.01139	0.00239	−0.0011483	
259	0.20235	0.08895	0.0000720	(−)275
227	0.47041	0.22658	0.0000426	
218	0.27468	0.12751	0.0000294	
217	0.05907	0.01891	−0.0000059	
206	0.47566	0.21157	−0.0002159	
201	0.00358	0.00943	−0.0000994	
Melatonin + (H <sub>2</sub> O) <sub>10</sub> <sup>c</sup> (Fig. 17)				
302	0.00106	0.00885	−0.0001029	(+)302
290	0.01142	0.00192	−0.0013072	
258	0.23991	0.12245	0.0000194	(−)275
226	0.40851	0.18640	0.0001108	
217	0.41100	0.21111	−0.0000221	
204	0.46550	0.22175	−0.0001903	
203	0.03965	0.02505	−0.0000392	

<sup>a</sup> STO-6G(d,p),  $E = -758.064522$  hartrees, Grms = 0.0321063 hartrees/bohr; not optimized. Geometry from: <http://ep.llnl.gov/msds/pdb/pdb.html>.

<sup>b</sup> STO-6G(d,p),  $E = -1136.737888$ , Grms = 0.0000001, optimized.

<sup>c</sup> STO-6G(d,p),  $E = -1515.428074$ , Grms = 0.0007588.

The MCD ( $B/D$ ) intensities in bohr-magntons/(cm<sup>−1</sup>) are comparable to the previously studied case of serotonin [18] and the strong MCD band of tryptophan at 290 nm first reported by Djerassi's group [36]. The sign of the ( $B/D$ ) values is opposite to the MCD spectra according to the rigid-shift-model [5,6]. The MCD spectral features are similar to those of indole, 5-hydroxy-indole, serotonin and tryptophan but with a new feature due to the additional  $n \rightarrow \pi^*$  band of the amide group between 300 and 320 nm. The broad band between 260 and 320 nm does not show resolution of more than one positive MCD band in water solvent even using the derivative of the spectra in Fig. 3. Although CNDO/S-D results are semiempirical, the predicted pattern of two separate positive MCD bands at 317 and 286 nm

followed by a negative MCD band at 251 nm is in approximate agreement with experiment for all three calculations. The first calculation is for a geometry from the PDB structure and was not optimized. It will be seen that this conformation with the extended alkyl chain is at least 0.06 hartrees (>37 kcal/mole) higher in energy than other conformations in which the alkyl chain is bent, but this extended structure may result from packing forces in the PDB structure.

The second and third calculations refer to geometries optimized with a STO-6G(d,p) basis at the SCF level (polarization functions, but no correlation) after placing water molecules at five places: (1) near the indole N–H, (2) near the –O–CH<sub>3</sub>, (3) over the pi-ring, (4) near the amide N-lone-pair and (5) near the amide keto C=O, with an

additional 5 water molecules in the third calculation. The second and third calculations include relaxation of the PDB structure and solvation interactions with water molecules. The interaction with water molecules shifts all the bands of the PDB structure to the blue, with the largest effect on the amide  $n \rightarrow \pi^*$  transition. This can be understood by noting that in the gas phase the N-lone-pair is part of the amide  $\pi$ -electron system, but when that lone pair and/or the non-bonded electrons on the keto-O is H-bonded to a water molecule(s) the amide  $\pi$ -electron system is reduced in size to mainly the carbonyl group with a corresponding blue-shift. A similar effect occurs for all the other bands in that the chromophores require more energy to excite electrons partially attracted to H-bonds in the solvated case. Even so, the amide  $n \rightarrow \pi^*$  transition remains to the red of the 286 nm indole band and the overall agreement with the MCD band features is plausible.

In order to add credibility to the semiempirical CNDO/S-D results, the same subroutines were used in a Gaussian-lobe basis program PCLOBE [47] with the same limit of 99 singly-excited configurations, and a factor of 0.646 was used to scale the energies based on fitting the  $A_{1g} \rightarrow B_{2u}$  band of benzene at 262.53 nm [53]. Although highly detailed vibrational spectra of benzene was reported by Bernstein in 1970 [58], the earlier work used in the text by Harris and Bertolucci [53] enables evaluation of the 0–0 band for the  $A_{1g} \rightarrow B_{2u}$  electronic transition needed here. Even so, the calculated wavelengths using the ab initio (6G 1s/4G 2s/4G 2p) minimum basis are to the blue of the experimental bands and the CNDO/S-D calculated bands in Table 3. However, the signs and magnitude of the ( $B/D$ ) values generally agree with the CNDO/S-D values and with the experimental spectrum of indole in aqueous solution. This serves mainly to add credibility to the CNDO/S-D method as applied to the larger cases.

Two calculations are shown for indole associated with 2 water molecules. One merely has another water forming a short hydrogen-bond to a water molecule linked to the ring NH system. The second is constrained to be Cs symmetry with a water molecule above and below the plane of the indole ring system. These systems were optimized using

a STO-6G(d,p) basis and the final geometries were then used in the (6G 1s/4G 2s/4G 2p) Gaussian-lobe basis MCD calculations.

In Table 3 CNDO/S-D results are presented for a number of related compounds, and compared to our previous experimental results [18]. The structures of these molecules were optimized using the GAMESS program in a STO-6G(d,p) basis set and the final coordinates were used as input to the CNDO/S-D program. The geometry optimization was continued until the root-mean-square energy gradient reached the value given in Table 3 as Grms. The STO-6G(d,p) basis was chosen for speed of calculations for large molecules and because the CNDO/S-D calculations use a simulated STO basis set.

Although there are small shifts in the characteristic MCD band pattern of substituted indoles, the overall pattern of a large positive band near 290 nm followed by negative bands near 250 nm and then more positive bands near 210 nm remains largely constant whether surrounded by a polar solvent such as water or a nonpolar solvent such as hexane. The wavelengths, oscillator strengths and ( $B/D$ ) values are computed with the CNDO/S-D method using the same geometry as found from the STO-6G(d,p) optimization. The small red shift predicted for 5-hydroxy or 5-methoxy substitution of 3–5 nm was noted in previous work [18]. This shift due to 5-oxy substitution is predicted to be slightly larger than the several solvent shifts, but in Table 2 the full ab initio calculation shows solvent shifts of up to 4 nm. While these shifts are interesting, they are certainly within the uncertainty of the method due to the use of scaling relative to benzene.

In order to investigate at least the prediction of transition wavelengths, a potentially more accurate method than CIS is available in the GAUSSIAN98 program. The time-dependent formulation of density functional theory (TD-DFT) [44,45] proved to yield excitation energies that were closest to experiment in previous work [23]. The strength of this method is expected to be best for low energy transitions well below the ionization threshold of a given molecule. This is surely the case for the longest-wavelength transitions for indole and mela-



Table 2  
Ab initio MCD band assignments for indole (99 SCI)

Transition	eV	nm	0.646	$f(\text{len.})$	$f(\text{vel.})$	( $B/D$ )
Indole, $E = -359.9553037$ a.u. (6G 1s/4G 2s/4G 2p) basis						
1	6.919	179	277	0.04885	0.00582	−0.00101265
2	7.381	168	260	0.15067	0.02804	+0.00028745
3	9.515	130	202	0.21005	0.00988	+0.00089197
4	9.633	129	199	1.76981	0.29350	−0.00003370
Indole + H <sub>2</sub> O–H–N, $E = -435.5988914$ (6G 1s/4G 2s/4G 2p) basis (Fig. 6)						
1	6.891	180	279	0.06174	0.00692	−0.00099481
2	7.272	171	264	0.12983	0.02062	+0.00043243
3	9.398	132	204	0.22416	0.01147	+0.00039763
4	9.565	130	201	1.71827	0.28286	−0.00003492
Indole + H <sub>2</sub> O over pi-plane, $E = -435.5794734$ (6G 1s/4G 2s/4G 2p) basis						
1	6.972	178	275	0.04697	0.00594	−0.00082952
2	7.477	166	257	0.15716	0.02485	+0.00029567
3	9.662	128	199	0.27346	0.03745	+0.00121409
4	9.710	128	198	1.83523	0.34571	−0.00011713
Indole + 2H <sub>2</sub> O, $E = -511.2259173$ (6G 1s/4G 2s/4G 2p) basis						
1	6.967	178	276	0.05681	0.00698	−0.00093135
2	7.359	169	261	0.13711	0.02024	+0.00043506
3	9.603	129	200	0.26709	0.03227	+0.00071338
4	9.679	128	198	1.81487	0.34328	−0.00008128
Indole + 2H <sub>2</sub> O (Cs), $E = -511.2047834$ (6G 1s/4G 2s/4G 2p) basis (Fig. 7)						
1	7.173	173	268	0.06259	0.00991	−0.00089092
2	7.515	165	255	0.13935	0.01945	+0.00060909
3	9.805	126	196	2.25793	0.42059	+0.00000394
4	10.263	121	187	1.36111	0.23059	−0.00002753

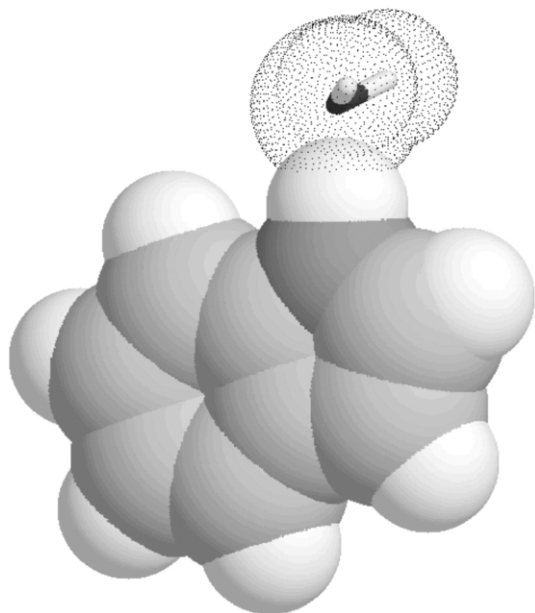


Fig. 6. Indole plus  $\text{H}_2\text{O}$  bound to N–H.

tonin, in which the lowest energy optical transitions are well below the ionization energy.

Here a small 6-31G\* (6-31G(d)) basis set was used for the estimation of ground state structures and excitation energies for indole and melatonin, but the B3LYP method should provide some electron correlation not present in the other SCF methods. Experience in this laboratory suggests that while this modest basis would probably yield plausible structures and (for melatonin) relative energies of conformers, a 6-311+G\*\* basis might make a substantial improvement in some transitions. The extent of this improvement is shown in some results for indole. The longest-wavelength transitions are shifted by approximately 0.2 eV or 1500 wave numbers when the basis is improved from 6-31G\* to 6-311+G\*\* (Frisch et al., [42]) to provide a flexible description of valence states. This shift was used to estimate the effect of the larger basis set with results from the mid-sized basis set as shown in Table 4. In the 6-311+G\*\* basis, transitions 4–7 proved to have negligible oscillator strengths and are not included in the table.

Melatonin can assume a number of conformations. The orientation of the methoxy fragment with respect to the ring N can be *syn* or *anti*. Torsion about the NC bond of the amide fragment, and the CC bonds linking the amide to the indole ring multiplies the number of possible low-energy conformers. This work follows a systematic nomenclature employed by Zwier [30], in which the alternatives are:

[*Anti* or *Gph* or *Gpy*]  
 × [*trans-in* or *trans-out* or *cis-in* or *cis-out*]  
 / *syn* or *anti*.

*Gph* and *Gpy* refer to gauche conformations around the Calpha–Cbeta bond with the amide N on the phenyl and pyrrole side, respectively. *Trans* and *cis* refer to the orientation of the C–Namide–Ccarbonyl–Cmethyl and -in and -out refer to the torsion around the Calpha–Namide bond. Finally, *syn* or *anti* refer to the orientation of the methoxy methyl relative to the ring N. Inspection of the figures will make the nomenclature clearer.

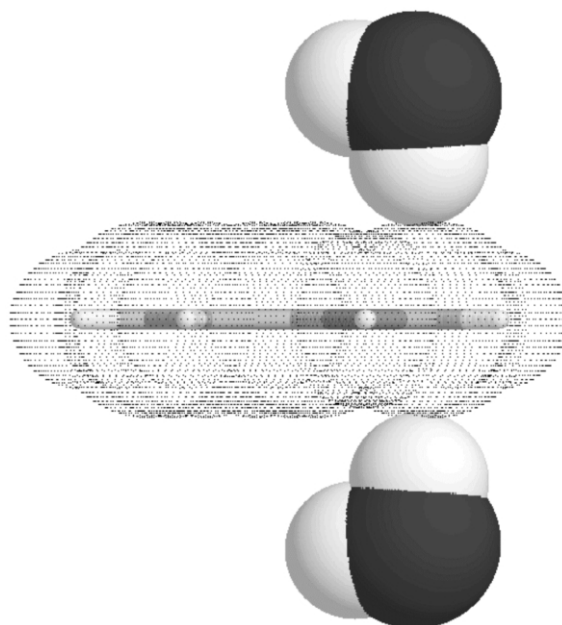


Fig. 7. Indole plus 2( $\text{H}_2\text{O}$ ),  $\text{C}_s$  symmetry.

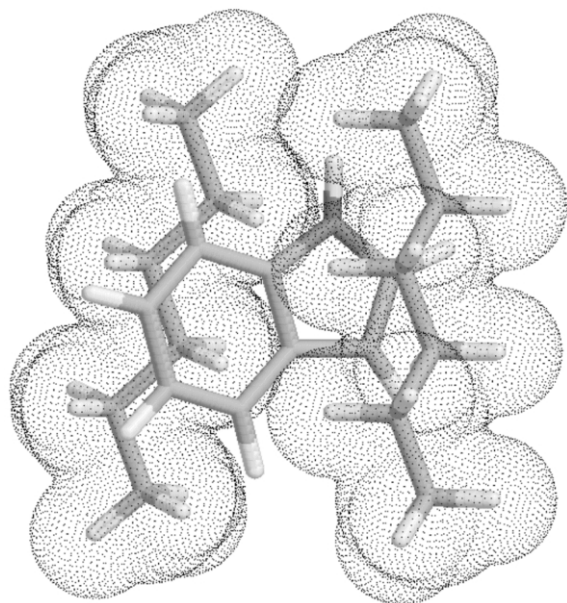
Table 3  
CNDO/S-D MCD band assignments for substituted indoles

nm	$f(\text{ZDO})$	$f(\text{d-vel})$	$(B/D)$ , B.M./cm	Experimental, nm
Indole, STO-6G(d,p), $E = -360.567004$ , Grms=0.0000001 hartree/bohr				
281	0.01065	0.00200	-0.0007013	
249	0.26964	0.09429	0.0000417	
219	0.26171	0.07560	-0.0000046	
210	0.39292	0.15613	0.0000563	
202	0.29083	0.08203	-0.0001573	
Indole + H <sub>2</sub> O on N-H, STO-6G(d,p), $E = -436.273695$ , Grms=0.0000000 (Fig. 6)				
281	0.00997	0.00231	-0.0008180	(+)287
248	0.30353	0.14269	0.0000402	(-)261
218	0.30146	0.12082	-0.0000141	
208	0.37454	0.17344	0.0001059	
201	0.48361	0.18936	-0.0001123	
Indole + (H <sub>2</sub> O) <sub>2</sub> pi + N-H, STO-6G(d,p), $E = -512.015335$ , Grms=0.0000004				
283	0.01537	0.00368	-0.0004182	(+)287
252	0.25235	0.10902	0.0000487	(-)261
219	0.37567	0.15823	-0.0000188	
211	0.33288	0.14909	0.0000908	
201	0.47156	0.16608	-0.0001434	
Indole + (hexane) <sub>2</sub> , STO-6G(d,p), $E = -830.436239$ , Grms=0.0000031 (Fig. 8)				
280	0.00814	0.00102	-0.0010619	(+)280
247	0.30835	0.14729	0.0000252	(-)265
215	0.30936	0.11593	-0.0000231	
207	0.40022	0.17139	0.0000766	
199	0.41036	0.12881	-0.0001969	
5-Hydroxyindole, STO-6G(d,p), $E = -435.123535$ , Grms=0.0000000				
287	0.02036	0.00425	-0.0002305	(+)296
251	0.22148	0.11055	0.0000316	(-)270
222	0.27612	0.08628	0.0000204	
215	0.64263	0.27738	0.0000491	
205	0.28177	0.10427	-0.0001807	(+)215
5-Methoxyindole, STO-6G(d,p), $E = -474.078022$ , Grms=0.00000002				
286	0.02278	0.00521	-0.0001100	
249	0.23784	0.11389	0.0000216	
220	0.28012	0.09544	0.0000185	
214	0.61180	0.28305	0.0000685	
205	0.34300	0.13688	-0.0001595	

Table 3 (Continued)

nm	$f(\text{ZDO})$	$f(\text{d-vel})$	$(B/D)$ , B.M./cm	Experimental, nm
Tryptophan PDB, STO-6G(d,p), $E = -680.169850$ , Grms = 0.0298487 <sup>a</sup> (Fig. 15)				
313	0.00149	0.00738	0.0000168	(+)288
281	0.00444	0.00022	-0.0003924	
251	0.30645	0.15042	-0.0000021	
236	0.00199	0.00156	-0.0002401	
219	0.18296	0.05939	0.0000728	
207	0.07501	0.02999	0.0000263	
203	0.00653	0.00675	-0.0000457	
200	0.43501	0.15095	-0.0001070	
Serotonin PDB, STO-6G(d,p), $E = -567.848261$ , Grms = 0.0280317 <sup>b</sup>				
286	0.00786	0.00116	-0.0003066	(+)296
254	0.25064	0.10404	0.0000142	
223	0.18726	0.05659	0.0000930	
212	0.18679	0.06797	-0.0000727	
207	0.03507	0.01624	-0.0000040	
204	0.12519	0.04453	0.0010816	
203	0.18918	0.05408	-0.0010607	
Serotonin + (H <sub>2</sub> O) <sub>10</sub> , STO-6G(d,p), $E = -1325.203870$ , Grms = 0.0001136				
288	0.02210	0.00493	-0.0003638	(+)296
252	0.23764	0.11563	0.0000466	
223	0.32186	0.07891	0.0000825	
220	0.47565	0.24092	-0.0000311	
205	0.36009	0.14826	-0.0001160	
202	0.07696	0.03946	-0.0001635	

<sup>a</sup> Geometry from: <http://ep.llnl.gov/msds/pdb/pdb.html>.<sup>b</sup> Geometry from: <http://ep.llnl.gov/msds/pdb/pdb.html>.

Fig. 8. Indole plus 2(*n*-hexane).

If all structures are comparable in energy, it appears there may be  $3 \times 4 \times 2 = 24$  distinct species. This estimate however assumes that the amide chain is always attached perpendicular to the ring plane. Zwier finds two low-lying conformers in which this is not the case [30]. The SPARTAN program permits an automatic listing of conformations, and a rank ordering of relative energies. The first efforts, seeking conformations within 5 kcal/mole of the *Anti(trans-out)/anti* species as estimated by fast STO-3G energy calculations in SPARTAN yielded 12 low-lying candidates. The set included the eight lowest energy species reported by Zwier's group [30] up to a relative energy of 3.0 kcal/mole according to their B3LYP and MP2

calculations) except for the two with side chains attached parallel to the rings.

A particularly interesting result of the investigation by Zwier and associates is that their jet-cooling traps five conformers, including two relatively energetic species. These apparently cannot relax quickly to the lowest energy forms. Here calculations were carried out for excitation energies for the five species they identify. The energy ordering is paired with the predicted MCD bands from the CNDO/S-D calculations for the corresponding coordinates in Table 5.

During the study of the conformers found by Zwier's group [30] it was observed that 1 water molecule might form a H-bond simultaneously to both the keto-O lone pair of electrons and also interact with the N–H region of the indole aromatic ring. This structure was found to be more stable than conformers with water bound to either site alone as given in Table 6. The pictures of this structure show the indole N–H bond bent toward the O-lone-pair of the solvent molecule as in Fig. 18. Therefore, an MCD spectrum of melatonin in methanol was obtained in order to test the hypothesis of the solvent-bridged conformer with methanol. Calculations were also carried out substituting a bridging methanol for the water bridge and reoptimizing the structure.

#### 4. Discussion and conclusions

The work described by Zwier's group [30] is truly wonderful in its detail for gas phase structures, but their conformers A–E may not apply directly to the solution structures. Their measurements place the lowest energy transitions for gas phase conformers A–E between 32 400 and 32 800/cm (between 308 and 305 nm,  $\sim 4.1$  eV)

Table 4  
TD-DFT transition energies of indole

	Basis = STO-6G**		Basis = 6-31G*		Basis = 6-311 + G**	
	Energy (nm)	<i>f</i>	Energy (nm)	<i>f</i>	Energy (nm)	<i>f</i>
Tr 1	5.695 (218)	0.0404	5.002 (248)	0.0471	4.701 (264)	0.0766
Tr 2	5.920 (209)	0.0365	5.138 (241)	0.0472	4.836 (256)	0.0350
Tr 3	7.299 (170)	0.3931	6.331 (196)	0.2991	4.875 (254)	0.0018
Tr 8					5.912 (210)	0.3901

Table 5

Energies and predicted MCD bands of melatonin conformers

Transition	eV	nm	<i>f</i>
TD-DFT transitions for conformer A (not scaled) <sup>a</sup>			
1	4.536	273	0.0608
2	4.888	254	0.0871
3	5.617	221	0.0019
4	5.708	217	0.0071
nm	<i>f</i> (ZDO)	<i>f</i> (d-vel)	( <i>B/D</i> ), B.M./cm
CNDO/S-D MCD for melatonin conformer A (Fig. 9)			
313	0.00043	0.00221	−0.0001580
294	0.01574	0.00391	−0.0004955
263	0.30691	0.14173	0.0000282
228	0.24934	0.08752	0.0000642
219	0.34005	0.17021	−0.0000077
208	0.47671	0.17560	−0.0001912
205	0.00147	0.00110	0.0000178
Transition	eV	nm	<i>f</i>
TD-DFT transitions for conformer A (not scaled) <sup>b</sup>			
1	4.518	275	0.0668
2	4.916	253	0.0833
3	5.263	236	0.0106
4	5.560	223	0.0182
nm	<i>f</i> (ZDO)	<i>f</i> (d-vel)	( <i>B/D</i> ), B.M./cm
CNDO/S-D MCD for melatonin conformer B (Fig. 10)			
307	0.00075	0.00378	−0.0000861
293	0.01542	0.00356	−0.0006663
261	0.30430	0.14032	0.0000282
227	0.23951	0.08118	0.0000658
219	0.33479	0.16729	0.0000018
209	0.51390	0.19543	−0.0001787
204	0.00377	0.00401	0.0014456
Transition	eV	nm	<i>f</i>
TD-DFT Transitions for conformer C (not scaled) <sup>c</sup>			
1	4.517	274	0.0588
2	4.857	255	0.0847
3	5.459	227	0.0172
4	5.589	222	0.0013
nm	<i>f</i> (ZDO)	<i>f</i> (d-vel)	( <i>B/D</i> ), B.M./cm
CNDO/S-D MCD for melatonin conformer C (Fig. 11)			
311	0.00027	0.00282	0.0000400
295	0.01239	0.00277	−0.0007969
265	0.29948	0.13313	0.0000254
230	0.27195	0.09693	0.0000799
220	0.32342	0.15772	−0.0000074
209	0.46837	0.17609	−0.0002012
205	0.00785	0.00687	0.0001351

Table 5 (Continued)

Transition	eV	nm	<i>f</i>
TD-DFT transitions for conformer D (not scaled) <sup>d</sup>			
1	4.551	272	0.0538
2	4.864	255	0.0846
3	5.537	224	0.0003
4	5.607	221	0.0018
nm	<i>f</i> (ZDO)	<i>f</i> (d-vel)	( <i>B/D</i> ), B.M./cm
CNDO/S-D MCD for melatonin conformer D (Fig. 12)			
315	0.00026	0.00208	−0.0001357
294	0.01590	0.00380	−0.0007542
263	0.31078	0.14407	0.0000235
228	0.23826	0.08070	0.0000068
219	0.33405	0.16755	0.0000390
210	0.50652	0.19641	−0.0002149
209	0.01280	0.00288	0.0024219
Transition	eV	nm	<i>f</i>
TD-DFT transitions for conformer E (not scaled) <sup>e</sup>			
1	4.493	276	0.0669
2	4.883	254	0.0841
3	5.353	232	0.0068
4	5.556	224	0.0028
nm	<i>f</i> (ZDO)	<i>f</i> (d-vel)	( <i>B/D</i> ), B.M./cm
CNDO/S-D MCD for melatonin conformer E (Fig. 13)			
310	0.00039	0.00240	0.0002766
287	0.01595	0.00392	−0.0004045
254	0.23836	0.11567	0.0000216
223	0.39377	0.18367	0.0000811
217	0.32286	0.15041	−0.0000111
212	0.05994	0.02216	0.0000608
205	0.40825	0.16912	−0.0001866

<sup>a</sup> Relative energy (B3LYP/6-31G\*)... 0.98 kcal/mole. Relative energy (Zwier B3LYP/6-31 + G(5d)) [−0.] kcal/mole.

<sup>b</sup> Relative energy (B3LYP/6-31G\*)... −0. kcal/mole. Relative energy (Zwier B3LYP/6-31 + G(5d)) [0.30] kcal/mole.

<sup>c</sup> Relative energy (B3LYP/6-31G\*)... 0.89 kcal/mole. Relative energy (Zwier B3LYP/6-31 + G(5d)) [0.69] kcal/mole.

<sup>d</sup> Relative energy (B3LYP/6-31G\*)... 1.93 kcal/mole. Relative energy (Zwier B3LYP/6-31 + G(5d)) [2.92] kcal/mole.

<sup>e</sup> Relative energy (B3LYP/6-31G\*)... 3.64 kcal/mole. Relative energy (Zwier B3LYP/6-31 + G(5d)) [3.25] kcal/mole.

so TD-DFT calculations with the small 6-31G\* basis overestimates the transition energies by approximately 0.4 eV or 10%. One might expect an improvement by approximately 0.2 eV with extending the basis to 6-311 + G\*\*. Although the full ab initio CIS method in Table 2 needs to be scaled just as the CNDO/S-D method, there is qualitative agreement between the two methods to show that the CNDO/S-D method gives results about what would be expected from the full ab

initio method. It should also be clear that shifts due to solvent effects are small and the main effects are for conformational changes. It can be noted that the presence of water in the calculation for melatonin in an extended conformation with 5 water molecules shows only small shifts compared to the unsolvated case. However, it is very interesting that when 10 water molecules are added the water molecules form H-bonded chains in such a way as to support conformations in which the

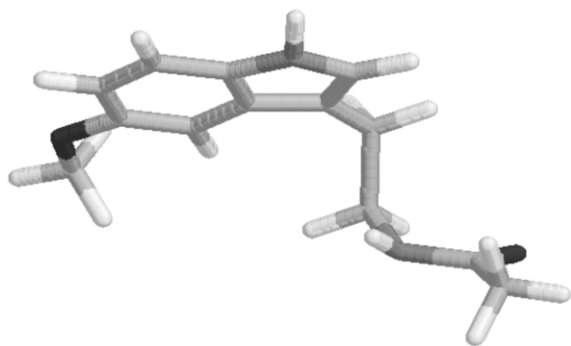


Fig. 9. Conformation A of melatonin.

alkyl chain is nearly perpendicular to the aromatic rings. This work infers that the aromatic portion of the melatonin molecule is more hydrophobic than the alkyl chain due to amide and keto groups in the alkyl chain. Thus the indole moiety would be solvated least by water and then only after water molecules form H-bonds to the indole N–H, the  $-\text{OCH}_3$ , the amide N-lone-pair and the amide keto-C=O regions. Adding more water molecules to the calculation merely forms linked H-bonded structures between such groups.

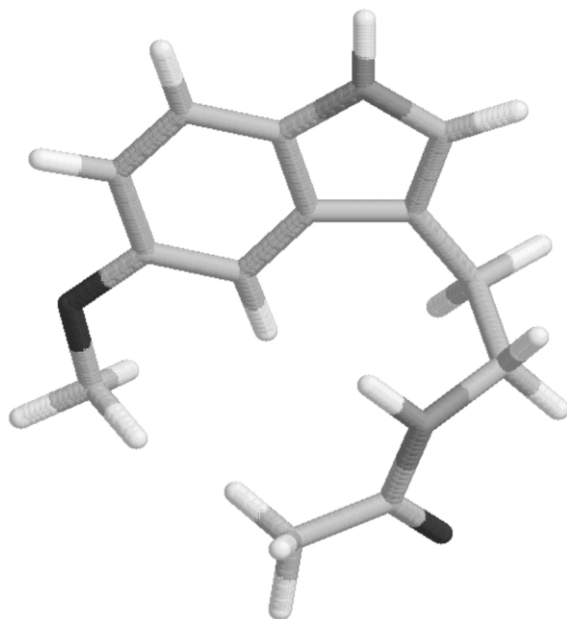


Fig. 11. Conformation C of melatonin.

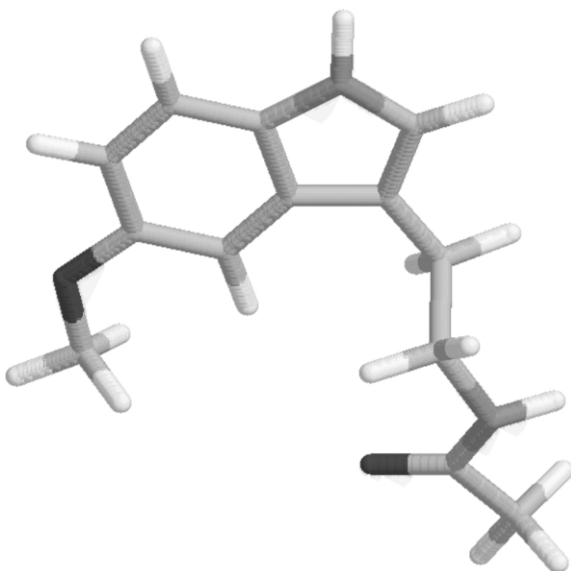


Fig. 10. Conformation B of melatonin.

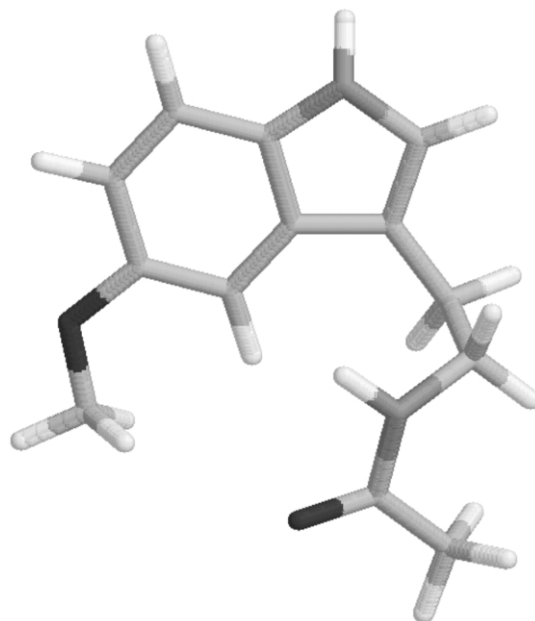


Fig. 12. Conformation D of melatonin.



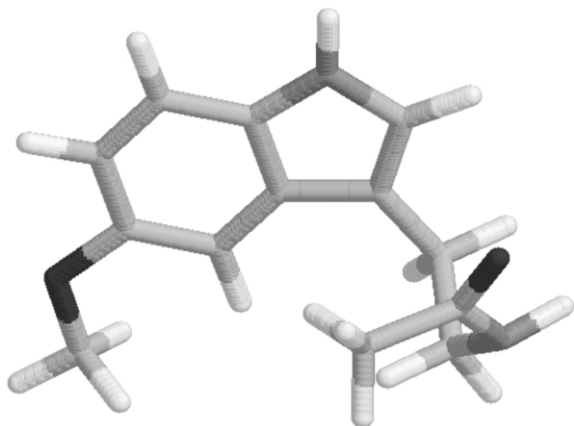


Fig. 13. Conformation E of melatonin.

There is a slight discrepancy here as to whether conformer A or B is the lowest energy using a smaller 6-31G\* basis but with inclusion of some correlation energy using the B3LYP local density approximation. Further calculations using a larger basis set still give the order shown here with the energy of conformer A as  $-765.1969344$  hartrees and the energy of conformer B as  $-765.1979540$  hartrees using the B3LYP method of GAUSSIAN98 with a 6-311++G basis set and optimizing to 0.0003 hartrees/bohr root-mean-square gradient. Using Zwier's geometries, at the B3LYP/STO-6G(d,p) level with GAMESS the lowest-energy conformer was E, followed by C, A, D, B and the

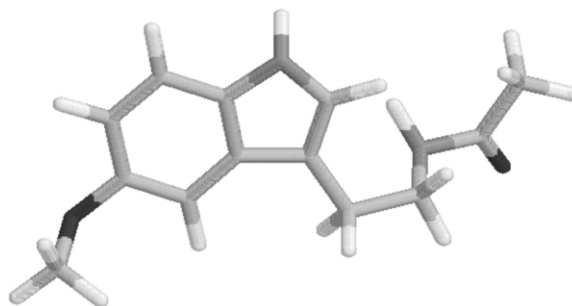


Fig. 14. PDB conformation of melatonin.

PDB structure. At the B3LYP/6-31+G(d,p) level the energies were, from lowest to highest, A, B, E, C, D and PDB. Perhaps we misunderstand the geometry of conformer A in Zwier's paper [30] so we show the structures labeled as we found them but they seem to be the same as Zwier has labeled (a)–(e) except we find (b) to be the lowest energy. However, A and B conformers are close in energy and both may be accessible with approximately 0.6 kcal/mole thermal energy at room temperature or with slightly more energy at 37 °C and both agree qualitatively with the pattern of signs in the experimental MCD spectra of melatonin in water.

Conformer C is only slightly higher in energy than A or B but the sign of the MCD band is opposite to the experimental spectra for the longest wavelength amide  $n \rightarrow \pi^*$  transition. There is no

Table 6  
B3LYP/6-31G\* results for water-bridged melatonins

Water-bridge structure	$-841.4065465$ a.u.			
Unbridged NH–H <sub>2</sub> O	$-841.4029969$ a.u.			
Amide carbonyl–H <sub>2</sub> O	$-841.4046310$ a.u.			
Conformer B alone	$-764.9822791$ a.u.			
nm	$f(\text{ZDO})$	$f(\text{d-vel})$	(B/D), B.M./cm	Experimental, nm
CNDO/S-D bands for the water-bridged-structure (Fig. 18)				
298	0.01457	0.00165	$-0.0005460$	(+)302
297	0.00074	0.00850	$-0.0000975$	
270	0.27251	0.11997	0.0000242	(–)275
238	0.02408	0.01392	0.0001171	
232	0.24545	0.08743	0.0000551	
220	0.27605	0.14112	0.0000792	
212	0.41092	0.14090	$-0.0002581$	
203	0.10815	0.06293	0.0001207	

sign of a negative band to the red of 300 nm so Conformer C and especially the higher energy Conformer E do not match the experimental spectrum very well.

Conformer D yields MCD bands compatible with the experimental spectrum, but for conformer D the energy is calculated to be approximately 2–3 kcal/mole above A or B.

Conformer E has a pattern of the computed MCD bands with the amide  $n \rightarrow \pi^*$  band opposite to the band at 287 nm, and the energy of conformer E is 3 kcal/mole or more above the lowest energy of conformers A and B.

Note that all five conformers A–E have at least one positive MCD band in the region from 287 to 295 nm, so that they are roughly compatible with the experimental spectrum. However, conformer E is least likely to be present since conformers A–D are predicted to have bands in the range of 293–295 nm compared to a shorter wavelength of 287 nm for conformer E, and E is much higher in energy than A or B.

Since the CNDO/S-D results are semiempirical and scaled by the 0.585 factor for  $\pi^*$  orbitals, one might expect only qualitative agreement with experimental spectra. However, it is striking that the experimental MCD spectrum of melatonin in water has a featureless band near 300 nm with only one peak in the derivative plot while the spectrum of melatonin in methanol shows two distinct bands in that region. If one gives the CNDO/S-D results in Table 6 the credibility of a well-calibrated empirical method [21], it appears that the water-bridged complex of water and melatonin produces the first two bands nearly degenerate at 296 and 297 nm with little chance of observing this splitting with the 1 nm resolution in the spectra presented here. The B3LYP energies in Table 6 and the experimental MCD spectra infer that the water-bridged structure shown in Fig. 18 is the main conformation of melatonin in water.

This melatonin and water structure, which has a single water molecule bridging the amide-keto oxygen and the indole-moiety N–H, was further examined by adding 39 more water molecules around the structure and optimizing at the STO-6G(d,p) level. The new 153 atom structure was optimized until the RMS gradient was less than

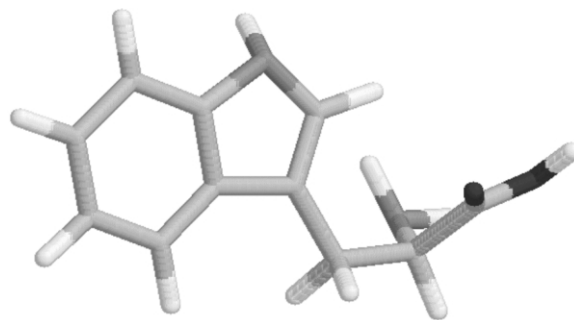


Fig. 15. PDB conformation of L-tryptophan.

$6 \times 10^{-4}$  hartree/bohr, and these coordinates were entered into the enlarged CNDO/S-D MCD program as the 410 valence electrons and 324 molecular orbitals could not be handled by our smaller ab initio MCD program.

The oxygen on the methoxy group and the nitrogen on the amide arm each had one water hydrogen bonded to them. A hydrogen on the methoxy group was bridged with a single water to a hydrogen on the methyl group of the arm, and the indole N–H had one water hydrogen bonded to each atom, one of these bonded to the oxygen on the amide arm in our proposed bridging structure. The remaining waters formed interlocking four-, five-, and six-membered rings with these waters around the melatonin molecule as shown in Fig. 21.

The first CNDO/S-D MCD peak was calculated to be at (+)287 nm, the second at (–)254 nm, and the third at (–)237 nm, using the benzene-calibrated 0.585  $\pi$ – $\pi^*$  scaling factor. This follows the trend of larger blue-shifts as the number of water or methanol solvent molecules around melatonin is increased. As shown in Table 6, this bridged structure optimized with only a single water molecule has CNDO/S-D MCD peaks calculated to be at (+)298, (+)297 and (–)270 nm.

Using a scaling factor that fits the first calculated melatonin with 40 waters peak to the experimentally-observed (+)302 nm value, the second peak would then be at (–)268 nm, vs. the measured (–)275 nm. This is consistent, as shown in Table 3Table 7, with CNDO/S-D calculating the first

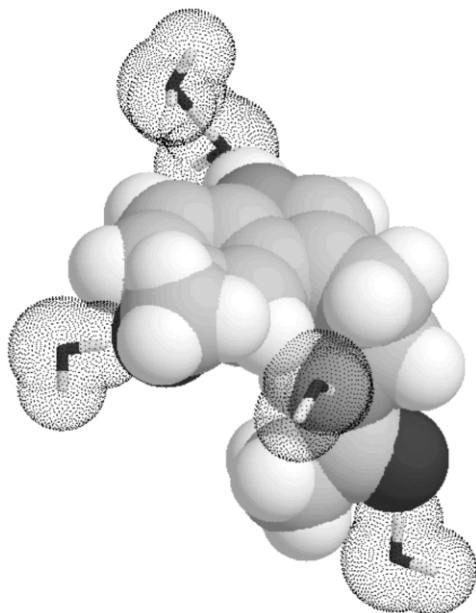


Fig. 16. Conformation of melatonin plus 5(H<sub>2</sub>O).

negative peak at a wavelength below that observed experimentally. For this semiempirical method, however, our error of less than 5% is quite satisfying. Although one might use a dielectric bath to simulate the bulk solvent, this work takes the direct approach of adding more solvent molecules to simulate the bulk solvent. We note that adding more water molecules does not add additional splitting to the MCD band near 300 nm; thus maintaining agreement between the experimental spectra and the results obtained using only 1 water molecule. We believe that a simulation with 40 water molecules and a calculation of MCD bands using 410 valence electrons in 324 molecular orbitals is at the forefront of current technology. Of course this is only one of many local minima in the energy hypersurface, but the simulation is sufficiently large to indicate that the interpretation from the case with only 1 water molecule remains valid.

Methanol can also form a H-bond to the amide keto-O (the most electronegative site among nearby options), but the methyl group may interfere with a bond to the indole N–H so that a methanol-bridged structure is less stable for melatonin in

methanol. The spectrum in Fig. 4 reveals a shoulder on the long wavelength edge and the derivative of the spectrum as shown in Fig. 5 clearly shows the presence of two bands near 300 nm in methanol. In Table 7 the second set of calculated MCD bands for the structure found here by Trindle for a bridging water molecule is treated with a bridging methanol molecule and reoptimized. Clearly this structure does not survive in methanol because the first two bands are the wrong sign and shifted too far to the blue of the observed bands.

Many other structures of melatonin interacting with one or several methanol molecules were considered and only a few are shown in Table 7. At this time the results show mainly that the alkyl-amide arm is extended away from the indole moiety when melatonin is solvated in methanol.

The chemical interpretation postulated here is that the water-bridged structure in Fig. 18 is a major conformer in aqueous solution. In methanol only an extended alkyl-amide group conformation, such as in the PDB structure, predict CNDO/S-D MCD bands similar to the experimental spectra. While this interpretation is certainly subject to the uncertainties of the semiempirical method, the

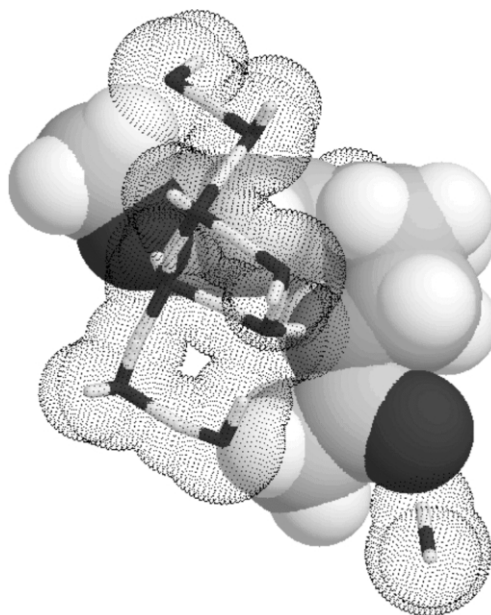


Fig. 17. Conformation of melatonin plus 10(H<sub>2</sub>O).

Table 7  
CNDO/S-D MCD band assignments for melatonin in CH<sub>3</sub>OH

nm	<i>f</i> (ZDO)	<i>f</i> (d-vel)	( <i>B</i> / <i>D</i> ), B.M./cm	Experimental, nm
Melatonin B + one methanol on N–H indole <sup>a</sup> (Fig. 19)				
298	0.00056	0.00230	−0.0000753	(+)310
287	0.01478	0.00274	−0.0006892	(+)303
255	0.25071	0.13345	0.0000445	(−)275
224	0.39226	0.17594	0.0000589	
216	0.37469	0.20586	0.0000168	
206	0.08383	0.04464	−0.0002270	
204	0.51220	0.25538	−0.0001547	
Melatonin with methanol in bridged-structure <sup>b</sup>				
287	0.01604	0.00477	0.0000958	
255	0.28823	0.16550	0.0000052	
235	0.01459	0.00672	−0.0000493	
222	0.26188	0.08952	0.0001438	
214	0.46448	0.26097	−0.0000206	
203	0.42197	0.20401	−0.0001683	
Methanol-bridged melatonin + four methanol molecules <sup>c</sup>				
285	0.01295	0.00388	−0.0000346	
255	0.25398	0.14299	0.0000051	
245	0.03952	0.02998	0.0000143	
225	0.01555	0.03784	0.0000109	
221	0.20800	0.06000	0.0001415	
214	0.49552	0.28055	0.0000252	
209	0.06445	0.02635	−0.0000889	
203	0.35029	0.16465	−0.0001780	
Melatonin + ten randomly oriented methanol molecules <sup>d</sup>				
287	0.02134	0.00486	−0.0004605	
252	0.25371	0.13636	0.0000277	
237	0.00519	0.01117	0.0001001	
222	0.36532	0.16141	0.0000587	
220	0.00259	0.00022	0.0008490	
216	0.40804	0.23027	0.0000116	
204	0.63943	0.32032	−0.0001300	
Melatonin with perpendicular alkyl-amide + one methanol molecule <sup>e</sup>				
297	0.00068	0.00314	−0.0000744	(+)310
288	0.01618	0.00301	−0.0009557	(+)303
253	0.26387	0.14296	0.0000608	(−)275
223	0.38982	0.17492	0.0000696	
216	0.44952	0.24165	−0.0000103	
203	0.55466	0.27825	−0.0001754	
Melatonin PDB + one methanol complexed to the amide group <sup>f</sup> (Fig. 20)				
310	0.00045	0.00150	−0.0003882	(+)310
289	0.02159	0.00591	−0.0004201	(+)303
252	0.22553	0.20140	0.0000704	(−)275
223	0.40810	0.19927	0.0000219	
217	0.40935	0.18338	0.0000335	

Table 7 (Continued)

nm	$f(\text{ZDO})$	$f(\text{d-vel})$	$(B/D)$ , B.M./cm	Experimental, nm
205	0.45238	0.01192	−0.0001790	

<sup>a</sup> STO-6G(d,p),  $E = -872.820117$ , Grms = 0.0001076.<sup>b</sup> STO-6G(d,p),  $E = -872.8134546332$ , Grms = 0.0003198.<sup>c</sup> STO-6G(d,p),  $E = -1331.5142220008$ , Grms = 0.0014060.<sup>d</sup> STO-6G(d,p),  $E = -1904.8945248236$ , Grms = 0.0003829.<sup>e</sup> STO-6G(d,p),  $E = -872.8019648410$ , Grms = 0.0007672.<sup>f</sup> STO-6G(d,p),  $E = -872.7985341949$ , Grms = 0.0003790.

implication is clear that in aqueous solution the water bridged structure is favored because it is stabilized by two interactions with a water molecule. Apparently the energy of the double interaction with the bridging water molecule stabilizes a compact form of conformer B more than that can occur with a single H-bond to other sites. This is supported by energy calculations in Table 6. Simple laboratory models show that conformer B needs but little distortion to form the bridged structure if the amide N–H rotates away from the indole plane and the calculations here show conformer B is the lowest energy gas phase structure. In methanol, the sites which can H-bond still can

do so with methanol, but the bridged structure is hindered by the methyl group of the solvent. The CNDO/S-D MCD calculations show that the methanol bridged structure in Table 7 gives the wrong sign of the first two MCD bands and a wavelength that is too far to the blue; clearly the bridged structure is not highly probable in methanol. Therefore, the CNDO/S-D model may be more reliable than supposed, at least for aromatic compounds similar to the calibration on benzene [19,21,37].

Other factors in the conformational analysis are the effect of entropy in aqueous solution and high energy barriers separating local energy minima. In the jet-cooled experimental data [30] the temper-

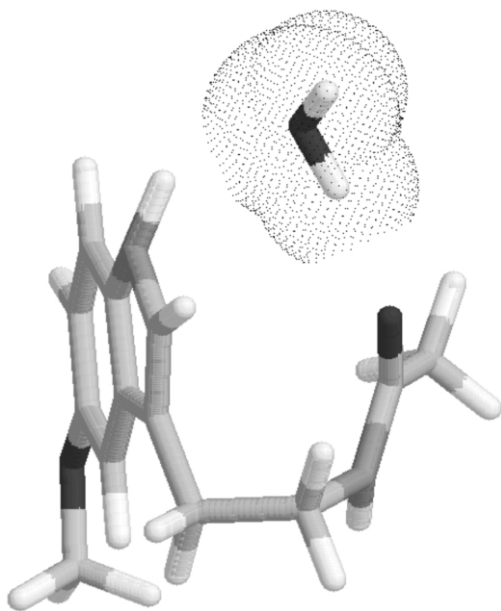


Fig. 18. Conformation of melatonin plus H<sub>2</sub>O bridge, note ring N–H bent toward O-lone-pair.

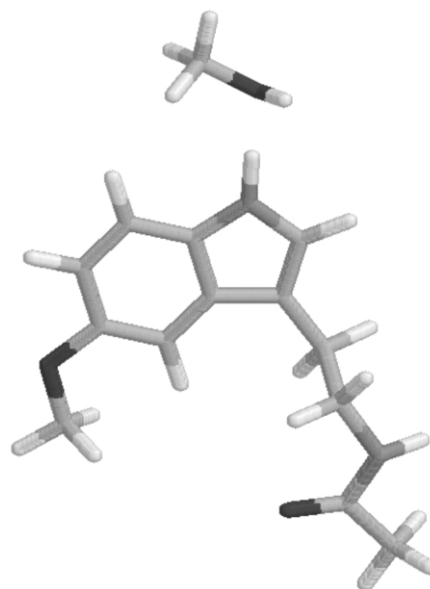


Fig. 19. Conformation B of melatonin plus one methanol on indole N–H.

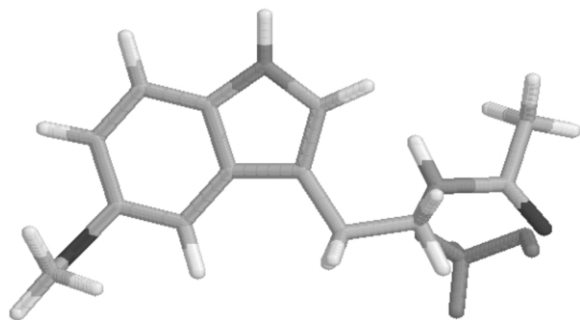


Fig. 20. PDB conformation of melatonin plus one methanol molecule.

atures are less than 50 K so that conformations from crystal structures may not have sufficient energy to equilibrate in the gas phase and become trapped in local energy minima. On the other hand, in aqueous solution at 37 °C, RT can be 0.616 kcal/mole to permit equilibration over a number of possible conformations. However, this is biased by two other factors, namely the maximization of entropy which favors extended conformations with maximum interaction of H-bonding sites and aqueous solvent and perhaps offset by internal H-bonds linking H-bonding sites with short chains of water to other H-bonding sites which favors non-extend-

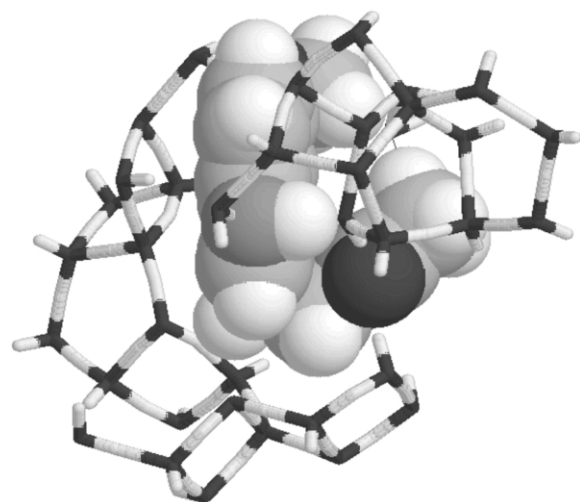


Fig. 21. Conformation of melatonin plus 40(H<sub>2</sub>O) at STO-6G(d,p), RMS gradient=0.0005343 hartree/bohr.

ed conformations. The net result implied here by energy calculations and analysis of the MCD band patterns is that the main conformation of melatonin in water is stabilized by 1 water molecule bridging the amide-keto oxygen and the distorted N–H of the indole ring. This may be a simple model system useful to calibrate molecular dynamics parameters intended to treat water molecules within protein structures.

### Acknowledgments

We want to thank Prof. Zwier for graciously sending us a preprint of work in press [30]. That highly detailed work stimulated this work to a great extent although differences between low temperature gases and aqueous solutions are noted above in terms of energy available to the species being studied. In addition we thank Prof. Sarah Rutan, the Principal Investigator of our project on solvation studies, for enabling us to carry out this project under a grant from the National Science Foundation: NSF CHE-0076290. Special thanks are also due to the Department of Chemistry of the University of Virginia for the use of the PQS PC-cluster in this work via NSF CHE-9807375, W.D. Harmon, P.I. Ms. Klonowski was supported by a GK-12 Virginia Interdisciplinary Science Graduate Teaching Fellowship in Middle School Education under NSF grant DGE-0086320. The calculated MCD spectra of the zwitterionic form of tryptophan has peaks at (–) 290, (+) 289, (+) 281 and (–) 264 NM, compared to the experimentally measured [18] (+) 288, (+) 281 and (–) 269 NM.

### References

- [1] W.J. Kauzmann, J.E. Walter, H. Eyring, Theories of optical rotatory power, *Chem. Rev.* 26 (1940) 339–407.
- [2] I. Tobias, W. Kauzmann, Faraday effect in molecules, *J. Chem. Phys.* 35 (1961) 538–543.
- [3] L. Rosenfeld, Quantenmechanische theorie der natürlichen optischen aktivitat von flussigkeiten und gasen, *Z. Phys.* 52 (1928) 161–174.
- [4] R. Serber, The theory of the Faraday effect in molecules, *Phys. Rev.* 41 (1932) 489–506.
- [5] P.J. Stephens, Theory of magnetic circular dichroism, *J. Chem. Phys.* 52 (1970) 3489–3516.

- [6] P.J. Stephens, P.N. Schatz, A.B. Ritchie, A.J. McCaffery, Magnetic circular dichroism of benzene, triphenylene and coronene, *J. Chem. Phys.* 48 (1968) 132–138.
- [7] E.U. Condon, Theories of optical rotatory power, *Rev. Mod. Phys.* 9 (1937) 432–457.
- [8] E. Gorin, W. Kauzmann, J. Walter, Optical activity of the sugars, *J. Chem. Phys.* 7 (1939) 327–338.
- [9] E. Gorin, J. Walter, H. Eyring, The optical activity of secondary butyl alcohol, *J. Chem. Phys.* 6 (1938) 824–832.
- [10] T.C. Kwoh, H. Eyring, Optical rotatory power of benzoin, *J. Chem. Phys.* 18 (1950) 1186–1192.
- [11] D. Stigter, J.A. Schellman, Approximations in the one-electron theory of optical rotation, *J. Chem. Phys.* 51 (1969) 3397–3403.
- [12] P.M. Bailey, E.B. Nielsen, J.A. Schellman, The rotatory properties of molecules containing two peptide groups: theory, *J. Phys. Chem.* 73 (1969) 228–243.
- [13] W. Kauzmann, *Quantum Chemistry*, Academic Press, New York, 1957, pp. 563–725.
- [14] I. Tinoco, R.W. Woody, Optical rotation of oriented helices. IV A free electron on a helix, *J. Chem. Phys.* 40 (1964) 160–165.
- [15] F.S. Richardson, D.D. Shillady, J.E. Bloor, The optical activity of alkyl-substituted cyclopentanones. INDO molecular orbital model, *J. Phys. Chem.* 75 (1971) 2466–2479.
- [16] F.S. Richardson, R. Strickland, D.D. Shillady, Optical activity of simple cyclic amides. INDO molecular orbital model, *J. Phys. Chem.* 77 (1973) 248–255.
- [17] D.D. Shillady, Ph.D. Thesis, The University of Virginia, Charlottesville, VA, 1970.
- [18] F.M. Sprinkel, D.D. Shillady, R.W. Strickland, Magnetic circular dichroism studies of indole, dl-tryptophan and serotonin, *J. Am. Chem. Soc.* 97 (1975) 6653–6657.
- [19] S. Baldwin-Boisclair, D.D. Shillady, An improved CNDO/S study of the circular dichroism of 1-methylindane in the 275–170 nm region, *Chem. Phys. Lett.* 58 (1978) 405–408.
- [20] J.A. Pople, The electronic spectra of aromatic molecules II: A theoretical treatment of excited states of alternant hydrocarbon molecules based on self-consistent molecular orbitals, *Proc. Phys. Soc. A* LXVIII (1955) 81–89.
- [21] J. Del Bene, H.H. Jaffe, Use of CNDO method in spectroscopy. I Benzene, pyridine, and the diazines, *J. Chem. Phys.* 48 (1968) 1807–1813.
- [22] N.R. Zhang, D.D. Shillady, Ab initio equilibrium constants for  $\text{H}_2\text{O}-\text{H}_2\text{O}$  and  $\text{H}_2\text{O}-\text{CO}_2$ , *J. Chem. Phys.* 100 (1994) 5230–5236.
- [23] C. Trindle, D. Shillady, J. Craig, S. Rutan, Dye probes of nanoclusters in liquids, *J. Clust. Sci.* 12 (2001) 473–486.
- [24] J.B. Fenn, Electrospray ionization mass spectrometry: how it all began, *J. Biomol. Tech.* 13 (2002) 102–107.
- [25] A. Held, D.W. Pratt, Hydrogen bonding in water complexes. Structures of 2-pyridone- $\text{H}_2\text{O}$  and 2-pyridone- $(\text{H}_2\text{O})_2$  in their  $S_0$  and  $S_1$  electronic states, *J. Am. Chem. Soc.* 115 (1993) 9708–9717.
- [26] J.A. Dickinson, P.W. Joireman, R.W. Randell, E.G. Robertson, J.P. Simons, Conformational structures of 3-phenyl-1-propionic acid, its *p*-hydroxy derivative and its hydrated clusters, *J. Phys. Chem. A* 101 (1997) 513–521.
- [27] M. Mons, I. Dimicoli, B. Tardivel, F. Piuze, V. Brenner, P. Millie, Site dependence of the binding energy of water to indole: microscopic approach to the side chain hydration of tryptophan, *J. Phys. Chem. A* 103 (1999) 9958–9965.
- [28] J.R. Carney, F.C. Hagemeister, T.S. Zwier, The hydrogen-bonding topologies of indole- $(\text{water})_n$  clusters from resonant ion-dip infrared spectroscopy, *J. Chem. Phys.* 108 (1998) 3379–3382.
- [29] J.R. Carney, T.S. Zwier, Infrared and ultraviolet spectroscopy of water-containing clusters of indole, 1-methylindole and 3-methylindole, *J. Phys. Chem. A* 103 (1999) 9943–9957.
- [30] G.M. Florio, R.A. Christie, K.D. Jordan, T.S. Zwier, Conformational preferences of jet-cooled melatonin: probing *trans*- and *cis*-amide regions of the potential energy surface, *J. Am. Chem. Soc.* 124 (2002) 10236–10247.
- [31] A. Bach, S. Leutwyler, Water-chain clusters: vibronic spectra of 7-hydroxyquinoline- $(\text{H}_2\text{O})_n$ ,  $n=1, 4$ , *Chem. Phys. Lett.* 299 (1999) 381–388.
- [32] R.E. Jacobs, S.H. White, The nature of the hydrophobic binding of small peptides at the bilayer interface: implications for the insertion of transbilayer helices, *Biochemistry* 28 (1989) 3421–3437.
- [33] D.W. Zaharevitz, R. Gussio, M. Leost, et al., Discovery and initial characterization of the paullones, a novel class of small-molecule inhibitors of cyclin-dependent kinases, *Cancer Res.* 59 (1999) 2566–2599.
- [34] S.P. Gunasekera, P.J. McCarthy, M. Kelly-Borges, Hamacanthins A and B, new antifungal bis indole alkaloids from the deep-water sponge, *Hamacantha* Sp, *J. Nat. Prod.* 57 (1994) 1437–1441.
- [35] Z. Varga, G. Panyi, M. Peter, et al., Multiple binding sites for melatonin on Kv1.3, *Biophys. J.* 80 (2001) 1280–1297.
- [36] G. Barth, R. Records, E. Bunnenberg, C. Djerassi, W. Voetler, Magnetic circular dichroism studies. XII. The determination of tryptophan in proteins, *J. Am. Chem. Soc.* 93 (1971) 2545–2547.
- [37] H. Dickerson, F.S. Richardson, Molecular orbital calculations on the optical activity of chiral benzene derivatives, *J. Phys. Chem.* 80 (1976) 2686–2693.
- [38] W. Pierpaoli, W. Regelson, Pineal control of aging: effect of melatonin and pineal grafting on aging mice, *Proc. Nat. Acad. Sci. USA* 94 (1994) 787–791.
- [39] W. Pierpaoli, W. Regelson, C. Colman, The Melatonin Miracle, Nature's Age-Reversing, Disease-Fighting, Sex-Enhancing Hormone, Simon and Shuster, New York, 1995.

- [40] R.J. Reiter, J. Robinson, *Your Body's Natural Wonder Drug: Melatonin*, Bantam Books, New York, 1995.
- [41] W. Hehre, W.W. Huang, *Chemistry with Computation: An Introduction to SPARTAN*, Wavefunction Inc, Irvine, CA, 1995.
- [42] M.J. Frisch, G.W. Trucks, H.B. Schlegel, et al., GAUSSIAN98, Revision A.11.3, Gaussian, Inc., Pittsburgh PA, 2002.
- [43] M.W. Schmidt, K.K. Baldridge, J.A. Boatz, et al., General atomic and molecular electronic structure system, *J. Comput. Chem.* 14 (1993) 1347–1363.
- [44] R. Bauernschmitt, R. Ahlrichs, Treatment of electronic excitations within the adiabatic approximation of time dependent density functional theory, *Chem. Phys. Lett.* 226 (1996) 454–464.
- [45] M.E. Casida, C. Jamorski, K.C. Casida, D. Salajub, Molecular excitation energies to high-lying bound states from time-dependent density-functional response theory: characterization and correction of the time-dependent local density approximation ionization threshold, *J. Chem. Phys.* 108 (1998) 4439–4449.
- [46] D.D. Shillady, F.P. Billingsley, J.E. Bloor, Valence shell calculations on polyatomic molecules IV. The effect of deorthogonalization on CNDO/2 dipole moments and charge distributions, *Theor. Chim. Acta (Berlin)* 21 (1971) 1–8.
- [47] D.D. Shillady, J. Craig, S. Rutan, Explicitly correlated SCF study of small hydrides, *Int. J. Quantum Chem.* 85 (2001) 520–528.
- [48] R.F. Stewart, Small Gaussian expansion of Slater-type orbitals, *J. Chem. Phys.* 52 (1970) 431–438.
- [49] H. Sambe, Use of 1s Gaussian wavefunctions for molecular calculations. I. The hydrogen atom and the hydrogen molecule ion, *J. Chem. Phys.* 42 (1965) 1732–1738.
- [50] I. Shavitt, The Gaussian function in calculations of statistical mechanics and quantum mechanics, in: B. Alder (Ed.), *Methods in Computational Physics*, vol. 2, Academic Press, New York, 1963, pp. 1–45.
- [51] E. Clementi, D.L. Raimondi, Atomic screening constants from SCF functions, *J. Chem. Phys.* 38 (1963) 2686–2689.
- [52] J.S. Rosenfield, A. Moscowitz, R.E. Linder, Vibronic magnetic rotational strengths in the B<sub>2u</sub> state of benzene, *J. Chem. Phys.* 61 (1974) 2427–2437.
- [53] D.C. Harris, M.D. Bertolucci, *Symmetry and Spectroscopy, An Introduction to Vibrational and Electronic Spectroscopy*, Oxford University Press, New York, 1978, pp. 388–389.
- [54] O. Sovars, W. Kauzmann, d-Hybridization of the pi bond in the 2p  $\Pi_u$  state of H<sub>2</sub><sup>+</sup>, *J. Chem. Phys.* 35 (1961) 652–655.
- [55] C.C.J. Roothaan, New developments in molecular orbital theory, *Rev. Mod. Phys.* 21 (1951) 69–89.
- [56] D.W. Ball, An introduction to magnetic circular dichroism spectroscopy: general theory and applications, *Spectroscopy* 6 (1990) 18–24.
- [57] H. Hug, G. Wagniere, Molecular orbital calculations of rotational strengths: a study of skewed diketones, *Theor. Chim. Acta (Berlin)* 18 (1970) 57–66.
- [58] E.R. Bernstein, Calculation of ground state vibrational structure and phonons of the isotopic benzene crystals, *J. Chem. Phys.* 52 (1970) 4701–4723.